ARGO-YBJ Experiment: review of results on Gamma-Ray Astronomy and Cosmic Ray Astrophysics

R. Assiro [1] , P. Bernardini [1 2] , A. Corvaglia [1], P. Creti [1], A. D'Amone [1 2], I. De Mitri [1 2], G. Mancarella [1 2], G. Marsella [1 3] , D. Martello [1 2], M. Panareo [1 3], L. Perrone [1 3], C. Pinto [1 2], S. Sbano [1 2], A. Surdo [1]

[1]Istituto Nazionale di Fisica Nucleare, sez. di Lecce, Italy

[2]Dipartimento di Fisica, Università del Salento, Italy

[3]Dipartimento di Ingegneria dell'Innovazione, Università del Salento, Italy

1. Introduction

The ARGO-YBJ [1] experiment is currently the only air shower array with a full-coverage active area operated at high altitude, with the aim of studying the cosmic radiation at an energy threshold of a few hundreds GeV. The large field of view ($\sim 2\,sr$) and the high duty cycle ($> 85\%$) allow a continuous monitoring of the sky in the declination band from -10° to 70° [2].

Crucial requirements for ARGO-YBJ to perform such studies are the operation stability, the pointing accuracy and the angular resolution. The performance of the detector and the operation stability are continuously monitored by observing the Moon shadow, i.e. the deficit of cosmic rays (CR) detected in its direction. Indeed, the size of the deficit allows the measurement of the angular resolution, while its position allows the evaluation of the absolute pointing accuracy of the detector. In addition, positively charged particles are deflected towards East due to the geomagnetic field by an angle depending on energy: $\Delta\theta \sim 1.6° Z/E[TeV]$. Therefore, the observation of the displacement of the Moon provides a direct calibration of the relation between shower size and primary energy. The Moon is observed with a sensitivity of about 9 standard deviations (s.d.) per month for events with a multiplicity $N_{pad} \geq 40$ and zenith angle $\theta < 50^o$ corresponding to a proton median energy $E_p \sim 1.8\ TeV$. The angular and energy resolutions are in good agreement with the expected values obtained by Monte Carlo analysis. In the energy range $(1-30)\ TeV$ the estimated energy uncertainty is smaller than 13%. The measured angular resolution is better than 0.5° for CR-showers of energies $E > 5\ TeV$ and is smaller by about $(30-40)\%$, depending on the multiplicity, for γ-rays due to the better defined time profile of the showers. The month analysis shows that the pointing accuracy is stable within 0.1^o while the angular resolution is stable at a level of 10%.

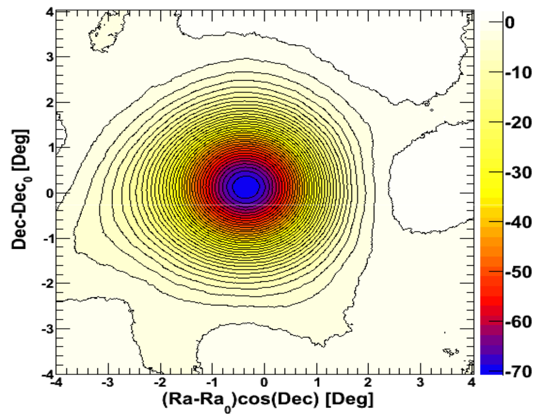

Figure 1. Moon shadow significance map for events with $N_{pad} \geq 40$ fired pads, observed by the ARGO-YBJ experiment in the period July 2006 - November 2010. The colour scale gives the deficit statistical significance in terms of s.d.

With all data from July 2006 to November 2010 ARGO-YBJ observed the CR Moon shadowing effect with a significance of about 70 s.d. (Fig. 1). The data analysis and a full account of the results are given in [3].

In the following sections the main results concerning gamma-ray source observations and cosmic ray astrophysics studies, achieved after about 3 years of data taking, are reviewed.

2. Gamma-Ray Astronomy

2.1. Localized gamma-ray sources

With about three years of data ARGO-YBJ observed 5 sources with a significance greater than 5 s.d.: Crab Nebula, Mrk421, MGRO J1908+06, MGRO J2031+41 and Mrk501.

The Crab Nebula. The Crab Nebula has been observed for 3.5 year (~ 1200 days) with a significance of 17 s.d. for $N_{pad} > 40$, without any event selection to reject hadron induced showers. According to MC simulations, 84% of detected events comes from primary photons of E $> 300\ GeV$, while only 8% comes from primaries

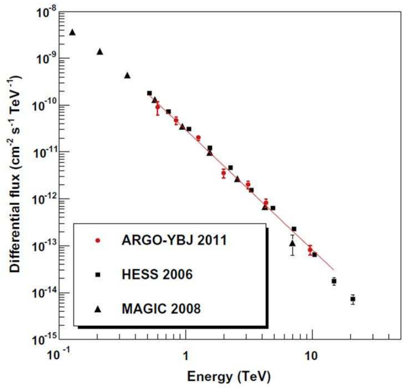

Figure 2. The Crab Nebula spectrum measured by ARGO-YBJ compared with the results of some other detectors. The reported erros are only statistical.

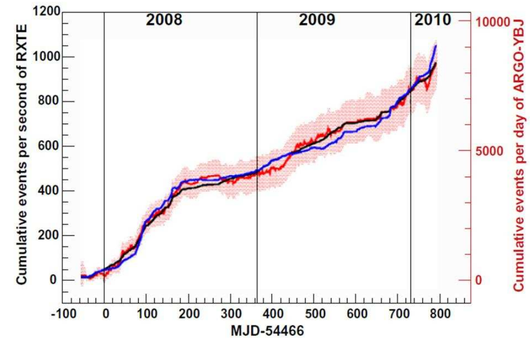

Figure 3. Cumulative light curve from Mrk421 measured by ARGO-YBJ (red curve) compared with RXTE/ASM (black) and Swift (blue) X-ray data. Shaded red region: 1σ statistical error.

above 10 TeV. The lowest point of the Crab spectrum shown in Fig. 2 is at a median energy $\sim 620\ GeV$. The observed flux is consistent with a steady emission and the observed differential energy spectrum in the $(0.3-30)\ TeV$ range is

$$dN/dE = (3.0 \pm 0.3) \times 10^{-11} \left(E/TeV\right)^{-2.57\pm0.09} \gamma/cm^2/s/TeV$$

in agreement with other measurements.
From these data we obtain that after 3 years of data taking the integrated sensitivity of ARGO-YBJ, without any rejection of the hadronic background, is of 0.3 Crab units.

The Crab showed a large γ-ray flare on September 18, 2010 reported by the AGILE and Fermi Collaborations [4,5]. A flux enhancement by a factor 4 in coincidence with this flare has beenobserved by ARGO-YBJ.

This flux variability has not been confirmed by the sparse observations of VERITAS (6 observations of about 20 mins each) and MAGIC (one observation of about 58 mins) during the duration of the flare. Thus, these results do not support the ARGO-YBJ findings. An increase of the flux (a 3.5 s.d. signal to be compared to an expected excess of 0.62 s.d.) has been also detected in coincidence with the flare detected by Fermi and AGILE in April 2011. No Cherenkov data are available for this event.

Finally, no evidence of a flux enhancement is observed during the flare detected by Fermi in February 2009.

The blazar Markarian 421.

Mrk421 is one of the brightest blazars and the closest to us ($z = 0.031$), characterized by a strong flaring activity with a variability time scale ranging from minutes to months, thus making the long term multiwavelength observation very important to constrain the emission mechanisms models. This AGN was the first source detected by the ARGO-YBJ experiment in July 2006 when the detector started recording data with only the central carpet. ARGO-YBJ has monitored Mrk421 for more than 3 years, studying the correlation of the TeV flux with X-ray data. We observed this source with a total significance of about 12 s.d., averaging over quiet and active periods. ARGO-YBJ detected different TeV flares in correlation with X-ray observations, as can be seen in Fig. 3 where the ARGO-YBJ cumulative events per day are compared to the cumulative events per second of the RXTE/ASM and Swift satellites. The X-ray/TeV correlation is quite evident over more than 3 years. The steepness of the curve gives the flux variation, that shows an active period at the beginning of 2008, followed by a quiet phase, and in February 2010.

The whole data set allows to study the relation between the flux and the TeV spectral index. The TeV flux measured by ARGO-YBJ ranges from 0.9 to about 7 Crab units. The TeV spectral index hardens with increasing flux in agreement with the results obtained by the Whipple collaboration in 2002. This conclusion generalizes the ARGO-YBJ result obtained with the analysis of the June 2008 flare [6]. The temporal and the spectral analysis strongly support the predictions of the one-zone SSC model. A full account of this analysis can be found in [7].

MGRO J1908+06.

With 3-years data ARGO-YBJ observed (significance $> 5\ \sigma$) this source discovered by Milagro in 2007 at a median energy of ~ 20 TeV and recently associated with the Fermi pulsar 0FGL J1907.5+0602. The data were consistent both with a point source and with an extended

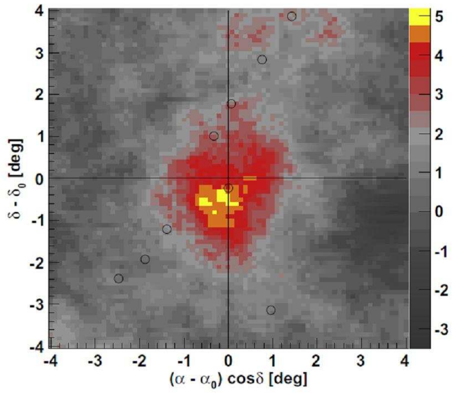

Figure 4. Significance map of the 8° × 8° region around MGROJ1908+06 by ARGO-YBJ, for events with $N_{pad} \geq 40$. The center of the map represents the position of the HESS source. The open circles show the positions of the gamma-ray sources observed by Fermi in the same region.

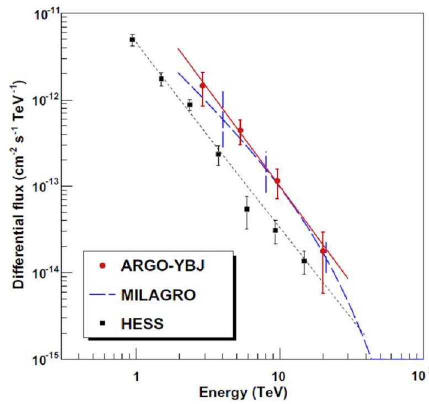

Figure 5. Differential flux from MGROJ1908+06 measured by different detectors: ARGO-YBJ (red circles, with best fit given by the continuous line); MILAGRO (blue dashed line); HESS (black squares). The plotted errors are purely statistical for the detectors.

source of diameter < 2.6°. HESS confirmed the discovery with the detection of the extended source HESS J1908+063 [8] at energies above 300 GeV, positionally consistent with the MILAGRO source. The extension of the source was extimated $\sigma_{ext} = 0.34°^{+0.04}_{-0.03}$. The MILAGRO and HESS fluxes are in disagreement at a level of 2-3 s.d., the MILAGRO result being about a factor 3 higher at 10 TeV [9].

ARGO-YBJ observed a TeV emission from MGRO J1908+06 with a significance greater than 5 s.d. in a total on-source time of 5358 hours, Fig. 4. At the ARGO-YBJ site, MGRO J1908+06 culminates at the relatively low zenith angle of 24° and is visible for 5.4 hours per day with a zenith angle less than 45°. By assuming a 2D Gaussian source shape with r.m.s = σ_{ext}, we fitted the event distribution as a function of the distance from the center (set to the HESS source position) and, taking into account the Point Spread Function (PSF), we found σ_{ext}=0.50±0.35, a value larger but consistent with the HESS measurement.

The best fit power law spectrum is: dN/dE = 2.2±0.4× 10^{-13} (E/7 TeV)$^{-2.3\pm0.3}$ photons cm^{-2} s^{-1} TeV^{-1} (the errors on the parameters are statistical) (Fig. 5).

A significant disagreement appears between the ARGO-YBJ and HESS fluxes. In the limit of the statistical accuracy of this result, our data support the MILAGRO measurement of a flux significantly larger than that measured by HESS. One possible cause of this discrepancy is that ARGO-YBJ and MILAGRO integrate the signal over a solid angle larger than the HESS one, and likely detect more of the diffuse lateral tail of the extended source. A contribution is expected from the diffuse gamma-ray flux produced by cosmic rays interacting with matter and radiation in the Galaxy. The amount of this contribution to the measured flux from MGRO J1908+06 at a few TeV is estimated (15−20)%, and cannot account for the entire observed disagreement.

MGRO J2031+41 and the Cygnus region.

The Cygnus region contains a large column density of interstellar gas and is rich of potential cosmic ray acceleration sites as Wolf-Rayet stars, OB associations and supernova remnants. Several VHE gamma-ray sources have been discovered within this region in the past decade,including two bright extended sources detected by the Milagro experiment.

The gamma ray source MGROJ2031+41, detected by MILAGRO at a median energy of $\sim 20 TeV$, is spatially consistent with the source TeV J2032+4130 discovered by the HEGRA detector and likely associated with the Fermi pulsar 1FGL J2032.2+4127. The extension measured by MILAGRO, 3.0° ± 0.9°, is much larger than that initially estimated by HEGRA (about 0.1°).

The bright unidentified source MGRO J2019+37 is the most significant source in the Milagro data set apart from the Crab Nebula. This is an enigmatic source due to its high flux not being confirmed by other VHE gamma-ray detectors. The Cygnus region has been studied by the ARGO-YBJ experiment by using data collected from 2007 November through 2011 August. The results of the data analysis are shown in Fig. 6 e Fig. 7 . A TeV emission from a position consistent with TeV J2032+4130/MGRO J2031+41 is found with a significance of 6.4 s.d.

The intrinsic extension of this emission results to be about 0.2°, a value consistent with the esti-

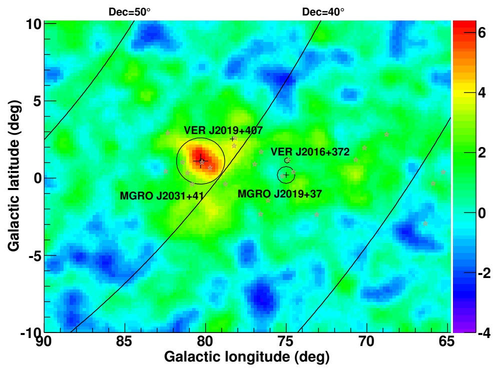

Figure 6. Significance map of the Cygnus Region as observed by the ARGO-YBJ experiment. The four known VHE γ-ray source are reported.

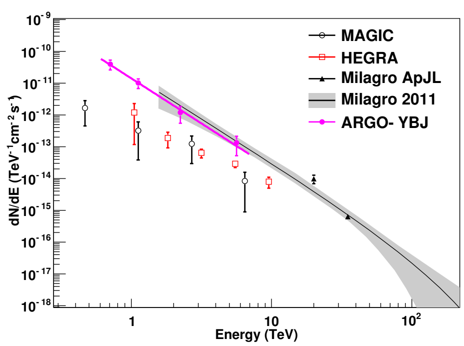

Figure 7. Energy density spectrum from TeV J2032+4130/MGRO J2031+41 as measured by the ARGO-YBJ experiment (magenta solid line). The spectral measurements of HEGRA [11] and MAGIC [12] are also reported for comparison.

mation by HEGRA [11] (and MAGIC [12]). Assuming σ_{ext}=0.1 the integral flux above 1 TeV is about 30% that of the Crab Nebula, which is much higher than the flux of TEV J2032+4130 as determined by HEGRA (5%) and MAGIC (3%).

The reason for the large discrepancy between the fluxes measured by Cherenkov telescopes and ARGO-YBJ is still unclear. Even considering a possible contribution from a diffuse emission spreading in the Cygnus region, it is difficult to explain this discrepancy.

On the contrary, no evidence of a TeV emission above 3 s.d. is found at the location of MGRO J2019+37. At energies above 5 TeV the ARGO-YBJ exposure is still insufficient to reach a firm conclusion while at lower energies the ARGO-YBJ upper limit is marginally consistent

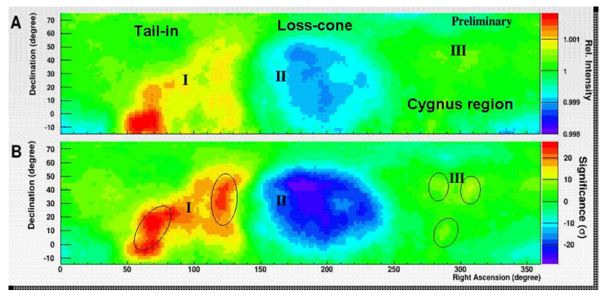

Figure 8. Large scale CR anisotropy observed by ARGO-YBJ. The color scale gives the relative CR intensity.

with the spectrum determined by Milagro. The observation of ARGO-YBJ is about five years later than that by Milagro. Given the estimated source radius of 4-15 pc, a flux variation over a smaller region in the source area cannot be completely excluded, such scenario, however, making impossible to identify MGRO J2019+37 as a pulsar wind nebula.

Markarian 501.

As an active blazar in the X-ray and TeV energy range, Mrk 501 is an excellent object for studying the physics associated with jets from AGNs. The ARGO-YBJ experiment has been monitoring it for γ-ray above $0.3 TeV$ since November 2007. Mrk 501 has been in a flaring activity since October 2011 and, even if preliminary, an excess greater than 6 s.d. is detected by ARGO-YBJ. The correlations between X-rays and γ-rays in both the GeV and TeV band are presently under investigation. To study the underlying mechanism of flaring, the wide energy range spectra during a quasi-steady period and the flare are investigated with a model based on synchrotron self-Compton processes. The hard spectral index -2.07 ± 0.21 during the flaring observed by ARGO-YBJ challenges the simple one-zone synchrotron self-Compton models and also provides a test bench for EBL models.

2.2. Diffuse emission from the Galactic Plane

Diffuse gamma rays are produced by relativistic electrons by bremsstrahlung or by inverse Compton scattering on background radiation fields, or by protons and nuclei via the decay of pai-zero produced in hadronic interactions with interstellar gases. Thus the space distribution of this emission can trace the location of the cosmic ray sources and the distribution of interstellar gases. Gamma rays at energies above 200 GeV near the

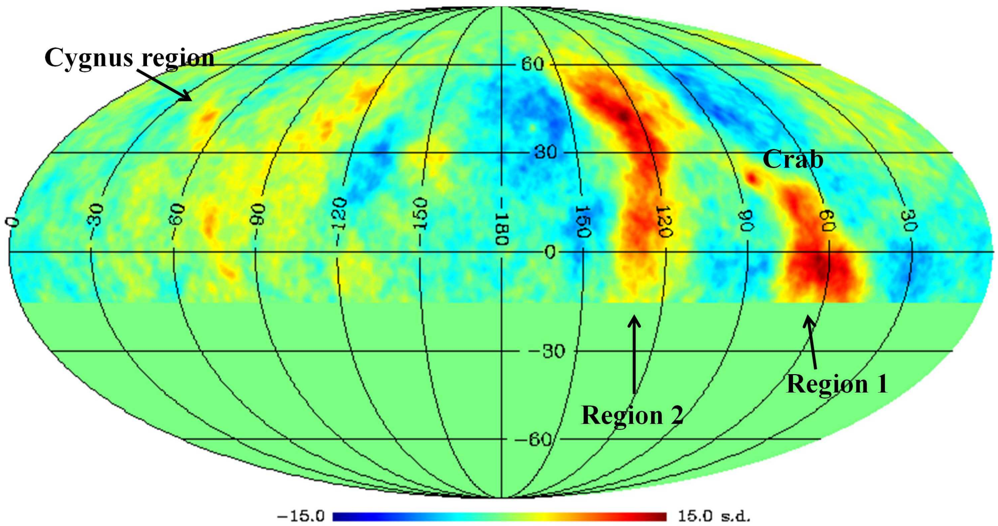

Figure 9. Medium scale CR anisotropy observed by ARGO-YBJ. The color scale gives the statistical significance of the observation in standard deviations.

Galactic center have been observed by the HESS telescope. A diffuse gamma ray flux at energies around 15 TeV from the $30° < l < 110°$ longitudine range of the Galactic plane has been reported by Milagro. A very preliminary analysis of the events collected by ARGO-YBJ in about 4 years of data taking evidences a diffuse emission at energies >300 GeV from the inner Galactic plane ($25° < l < 85°$,$|b| < 2°$) with a measured flux $E^2 \cdot dN/dE = 1 \div 1.5 \cdot 10^{-9}$.

3. Cosmic Ray Astrophysics

3.1. Observation of TeV Cosmic Ray anisotropies

Galactic Cosmic Rays at TeV energies are expected to appear highly isotropic, since during their propagation from the sources to the Earth they undergo complex processes, such as the deflection by the large scale Galactic magnetic field and the interaction with background photons and interstellar medium. However, extensive observations show that there exist a slight anisotropy of $\approx 10^{-3}$. In addition the relative intensity map of the cosmic ray flux exhibits some localized regions of significant excess in both hemispheres.

The observation of the CR large scale anisotropy by ARGO-YBJ is shown in the Fig.8. The data used in this analysis were collected by ARGO-YBJ from 2008 January to 2009 December with a reconstructed zenith angle $\leq 45°$. The so-called *'tail-in'* and *'loss-cone'* regions, correlated to an enhancement and a deficit of CRs, are clearly visible with a statistical significance greater than 20 s.d.. The tail-in broad structure appears to dissolve to smaller angular scale spots with increasing energy.

The Fig. 9 shows the ARGO-YBJ sky map in equatorial coordinates. The analysis refers to events collected from November 2007 to May 2011 after the following selections: (1) $\geq$25 shower particles on the detector; (2) zenith angle of the reconstructed showers $\leq$50°. The triggering showers that passed the selection were about $2 \cdot 10^{11}$. The zenith cut selects the declination region $\delta \sim$ -20°$\div$ 80°. According to the simulation, the median energy of the isotropic cosmic ray proton flux is $E_p^{50} \approx$1.8 TeV (mode energy $\approx$0.7 TeV).

The most evident features are observed by ARGO-YBJ around the positions $\alpha \sim 120°$, $\delta \sim 40°$ and $\alpha \sim 60°$, $\delta \sim$ -5°, positionally coincident with the regions detected by Milagro [10]. These regions, named "region 1" and "region 2", are observed with a statistical significance of about 14 s.d.. The deficit regions parallel to the excesses are due to a known effect of the analysis, that uses also the excess events to evaluate the background, artificially increasing the background. On the left side of the sky map, several possible new extended features are visible, though less intense than those aforementioned. The area $195° \leq R.A. \leq 315°$ seems to be full of few-degree excesses not compatible with random fluctuations (the statistical significance is more than 6 s.d. post-trial). The observation of these structures is reported here for the first time and together with that of regions 1 and 2 it may open the way to an interesting study of the TeV CR sky.

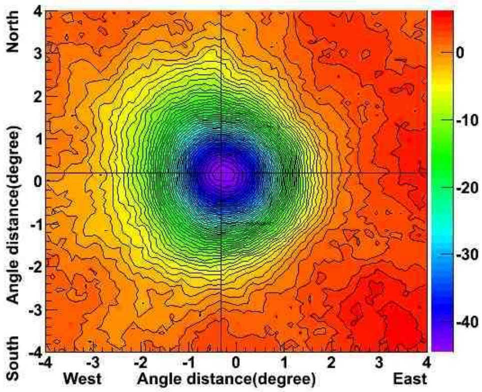

Figure 10. The Sun shadow measured using all the ARGO-YBJ data taken since July 2006 to October 2009. The maximum significance is 44.6 s.d. The step between contour lines is 1 s.d.

3.2. Interplanetary Magnetic Field measurement by Sun shadow

The same shadowing effect observed looking at cosmic rays in the direction of the Moon can be observed in the direction of the Sun, but the interpretation of this phenomenology is less straightforward. In fact, the displacement of the shadow from the apparent position of the Sun could be explained by the joint effects of the GMF and of the Solar and Interplanetary Magnetic Fields (SMF and IMF, respectively), whose configuration considerably changes with the phases of the solar activity cycle. Thus, understanding the Moon shadow phenomenology is a useful tool to disentangle the effect of different magnetic fields on the Sun shadow and to performe a measurement of the IMF in a minimum of the solar activity.

The observation using the ARGO-YBJ experiment was made just in such a particularly good time window when the solar activity stayed at its minimum for an unexpectedly long time since 2006. At distances greater than 5 solar radii from the sun centre, the IMF is distributed mainly in the ecliptic plane. Its z-component perpendicular to the ecliptic plane deflects cosmic rays in the east-west direction, therefore it drives the shadow with an extra shift in addition to the GMF effect which constantly moves the sun shadow towards west as observed in the moon shadow measurement. Its y-component, B_y, in the ecliptic plane defined to be perpendicular to the line of sight, deflects cosmic rays and thus drives the sun shadow in the north-south direction. It has no contamination from the GMF effect because the declination angle of the GMF is less than 0.5° at the ARGO-YBJ site.

The Sun shadow measured using all data taken by the ARGO-YBJ experiment from July 2006 to October 2009 is shown in Fig. 10. A detailed analysis has been carried out to study the shift of the center of the Sun shadow along the North-South direction as a function of the synodic Carrington longitude. The transverse component of the IMF, B_y, is then estimated with a minimal assumption on the model describing the IMF.

The B_y oscillates following a bi-sector or a four-sector pattern in two periods of data taking (period 1: from January 2008 to April 2009; period 2: all the other months from July 2006 to October 2009). These patterns depend on the direction of the IMF periods that causes the deflection of the particle trajectories. A positive sign is observed, which indicates that the field is pointing to the centre. The comparison to the measurements by the orbiting detectors (the corresponding data are available at http://omniweb.gsfc.nasa.gov) shows a good agreement after applying to the ARGO-YBJ data a phase shift of 21° corresponding to 1.6 days ahead. The two measurements are of the same order in amplitude (2.0±0.2 nT) and are consistent in the alternating periodical pattern. Since relativistic CRs fly from the Sun to the Earth in only 8 minutes, they are able to take an "instantaneous" picture of IMF pattern. On the contrary, the same information is transported by the solar wind at an average speed of about 400 km s^{-1} [13].

REFERENCES

1. R. Assiro *et al*, Annual Reports (*ARGO-YBJ Experiment in Tibet*) 2008 and 2010.
2. B. Bartoli *et al* (ARGO-YBJ Coll.), NIM A, vol. 659, 428-433 (2011).
3. B. Bartoli *et al* (ARGO-YBJ Coll.), Phys. Rev. D, vol. 84, 022003 (2011).
4. M. Tavani *et al.*, Science, **331**: 736-739 (2011).
5. A. A. Abdo *et al.*, Science, **331**: 739-742 (2011).
6. G. Aielli *et al* (ARGO-YBJ Coll.), The Astrophysical Journal, **714**: L208 (2010).
7. B. Bartoli *et al* (ARGO-YBJ Coll.), ApJ, vol. 734, p. 110 (2011).
8. F. Aharonian *et al.*, Astronomy and Astrophysics, **499**: 723-728 (2009).
9. A.J. Smith *et al.*, 2009 Fermi Symposium and eConf Proceedings C091122 (arXiv:1001.3695)
10. A.A. Abdo *et al.*, Physical Review Letters, **101** (2008) 221101-(1-5)
11. Aharonian, F. et al., Astronomy and Astrophysics, **431**: 197-202 (2005).
12. J. Albert *et al.*, The Astrophysical Journal, **675**: L25-L28 (2008).
13. G. Aielli *et al.*, The Astrophysical Journal, **729**: 113-116 (2011).